Plasma Response to a Varying Degree of Stress

Ami M. DuBois and Edward Thomas, Jr.
Department of Physics, Auburn University, Auburn, Alabama 36849, USA

William E. Amatucci and Gurudas Ganguli
Plasma Physics Division, Naval Research Laboratory, Washington, District of Columbia 20375, USA
(Received 11 June 2013; published 2 October 2013)

We report experimental evidence of a seamless transition between three distinct modes in a magnetized plasma with a transverse sheared flow as the ratio of the ion gyroradius to the shear scale length (a measure of shear magnitude) is varied. This was achieved using a dual plasma configuration in a laboratory experiment, where a sheared flow oriented perpendicular to a background magnetic field is localized at the boundary of the plasmas. This confirms the basic theory that plasma is unstable to transverse velocity shear in a broad frequency and wavelength range. The experiment characterizes the compression or relaxation of boundary layers often generated in a variety of laboratory and space plasma processes.

DOI: 10.1103/PhysRevLett.111.145002 PACS numbers: 52.25.Xz, 52.35.Qz, 52.72.+v

For a wide variety of laboratory and space plasma environments, theoretical predictions [1–3] state that plasmas are unstable to transverse and parallel inhomogeneous flows over a very broad frequency and wavelength range. A hierarchy of distinct modes of oscillation exists in a plasma in the presence of a transverse and/or a parallel sheared flow. Specifically, for a velocity shear oriented perpendicular to a uniform background magnetic field, the magnitude of the shear frequency (ω_s), as compared to the ion cyclotron frequency (ω_{ci}), determines the character of the shear driven instability that may prevail [3]. Since ω_s is inversely proportional to the shear scale length (L_s), $\omega_s \equiv dV/dx \sim 1/L_s$, the instabilities may also be characterized by a shear scale length compared to the ion gyroradius (ρ_i). For the first time, the continuous variation of the ratio ρ_i/L_s—and the associated transition of the instability regimes driven by the shear flow mechanism—is demonstrated in a single laboratory experiment under identical plasma conditions. This is a demonstration of the relaxation mechanism of compressed plasma layers in a collisionless plasma.

In the space plasma environment, sheared plasma flows have been observed by spacecraft in the ionosphere [4] and at boundaries such as the magnetopause [5,6] and the plasma sheet boundary layer [7–9]. Velocity shear is also generated in active experiments in space. For example, a region of electron depletion is created in the local plasma in the ionosphere by the release of electron capturing agents and at the boundary of the depletion, highly sheared electron flows develop [10–12]. Intense solar storms can compress and steepen the natural boundary layers. As boundary layers begin to relax from a compressed state and the ratio ρ_i/L_s decreases, observations of broadband electrostatic noise (BEN) have been reported, [6,13–17] in which the frequency range extends from below ω_{ci} up to the electron plasma frequency (ω_{pe}). Simulations [18] have confirmed that the free energy available in sheared electron flows can give rise to BEN spectra and can excite Kelvin-Helmholtz, ion cyclotronlike, and lower hybrid modes [1,19].

The kinetic theory described by Ganguli *et al.* [1–3] discusses three distinct instability regimes for transverse sheared plasma flows. For $\rho_i < L_s$, the low frequency Kelvin-Helmholtz instability [1] appears in the plasma with a characteristic frequency that is below ω_{ci}. Kelvin-Helmholtz instabilities [20–22] have long been studied in Q machines and more recently in the compact toroidal hybrid [23]. As L_s is decreased to become comparable to ρ_i, a different shear driven instability occurs near ω_{ci}. This instability mechanism is described as the inhomogeneous energy density driven instability (IEDDI) [1] and is distinct from the Kelvin-Helmholtz instability. Koepke *et al.* [24,25] and Amatucci *et al.* [26] have characterized the IEDDI when a magnetic field aligned current is also present in a Q machine. The IEDDI in a virtually nonexistent field aligned current has also been studied [27–30]. There exists a third mode when ρ_i becomes much larger than L_s, a regime in which electrons are magnetized in the shear layer, but the ions are effectively unmagnetized. The resulting shear driven instability occurs at a frequency well above ω_{ci} and closer to the lower hybrid frequency (ω_{LH}). This mode is known as the electron-ion hybrid (EIH) instability [2], which was experimentally characterized by Amatucci *et al.* [31], by Matsubara *et al.* [32], and by Kumar *et al.* [33]. All of these instabilities have a single free energy source, a transverse shear flow, but the physics of the energy extraction to support growth are different [2,34]. The ratio ρ_i/L_s acts as a surrogate for the magnitude of stress that the plasma layer is subjected to [13] and determines which mode is dominant. This ratio is also a convenient tunable experimental parameter that we exploit to induce the transition between the modes. While each of

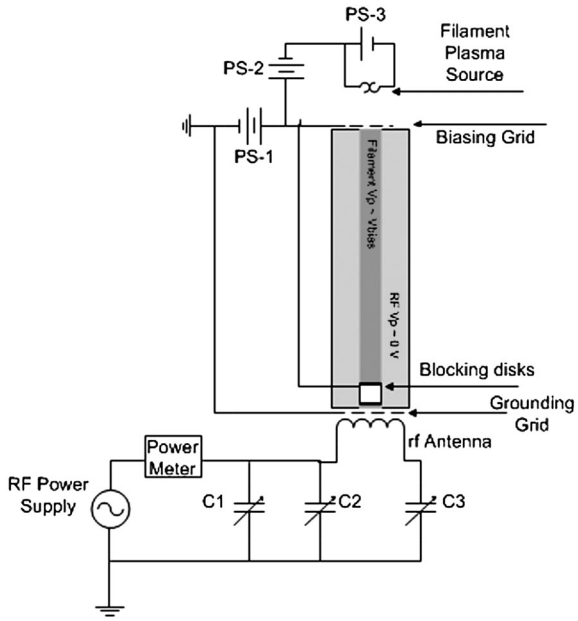

FIG. 1. A schematic of the experimental setup. A blocking disk creates a void in the rf plasma, which is filled in by a smaller diameter plasma from a hot filament source. The filament plasma potential is varied by PS-1 and PS-2 relative to the rf plasma potential, which is maintained at chamber ground. PS-3 resistively heats the filament source to thermionic temperatures.

these instability modes has been studied separately in different plasma experiments, no single experiment has shown the continuous transition from one mode to another to test how these different modes are interlinked with one another and produce BEN, which is the basis of the relaxation process [3] and is the primary objective of our experiment.

The experiments described in this Letter were performed using a double-plasma configuration in the Auburn Linear Experiment for Instability Studies (ALEXIS) [35–37] (shown in Fig. 1) and has been described previously [37]. Primary plasmas in ALEXIS are generated using a 13.56 MHz, 600 W radio frequency (rf) power supply. A matching network is used to couple the rf power from an antenna into the plasma. The secondary plasma source is a hot filament plasma source; i.e., it uses the thermionic emission of electrons from a heated wire to produce a plasma [38]. The secondary source consists of 3 separate parallel filaments made from tungsten. The filament source is designed to produce a plasma with a diameter of 2.5 cm. This is much smaller than the 10 cm diameter of the primary plasma source. Plasmas are generated using argon gas at a pressure of 0.3 mTorr with an input power of 40 W for the rf plasma and an emission current of 60 mA for the filament plasma. Electron densities range from 0.3 to 6×10^{15} m^{-3} with electron temperatures between 3 and 7 eV. The ion temperature is assumed to be room temperature.

A blocking disk is placed in front of the rf antenna to block out the central portion of the rf plasma. The smaller filament plasma then fills in this void, creating two interpenetrating plasmas. With this double plasma configuration, it is possible to control the electric field magnitude at the boundary between the two plasmas while preventing a parallel current from being introduced into the system.

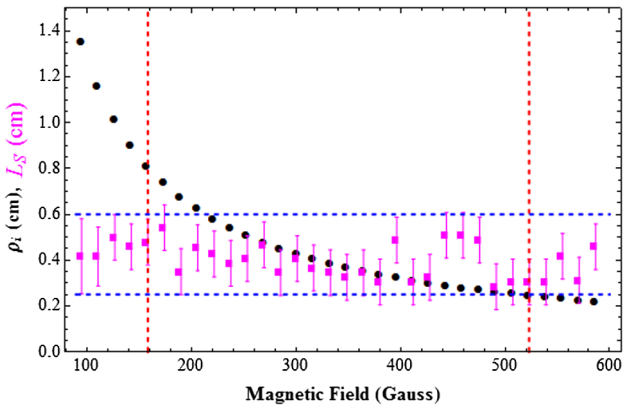

FIG. 2 (color online). ρ_i (circles, black) and the measured L_s (squares, pink) as a function of B_0. The dashed horizontal lines (blue) show the minimum and maximum measured L_s. The dashed vertical lines (red) indicate values of B_0 where a transition in the instability frequency is seen.

The goal of this study is to create a localized radial electric field and then vary ρ_i with respect to L_s by changing the magnetic field strength (B_0) to access the different instability regimes. An emissive probe is used to measure the plasma potential as the probe is moved radially across the plasma column. The electric field is then calculated from the plasma potential, and L_s is calculated from the half-width at half-maximum of the radial velocity shear profile. Figure 2 shows ρ_i (circles, black) and L_s (squares, pink) as a function of B_0. The dashed horizontal lines (blue) show the minimum and maximum measured L_s values. The measured values range from 0.25 to 0.6 cm, with an average of 0.4 ± 0.076 cm. For B_0 less than 160 G,

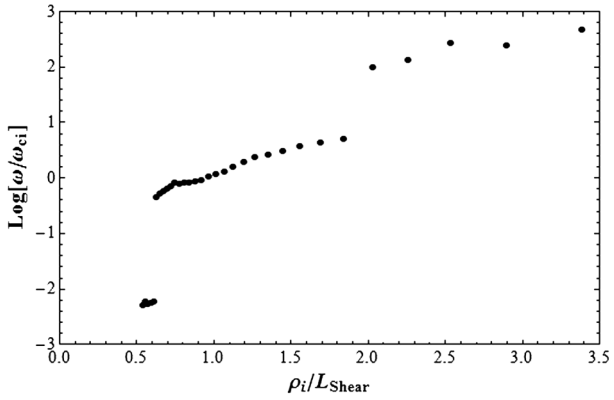

FIG. 3. The ratio of ω/ω_{ci} is plotted on a Log scale as a function of ρ_i/L_s. For a large ρ_i/L_s (low B_0) there is an instability with $\omega > \omega_{ci}$. For a small ρ_i/L_s (large B_0) $\omega < \omega_{ci}$. When $\rho_i \sim L_s$, the frequency is near ω_{ci}.

$\rho_i > L_s$. For B_0 greater than 520 G, $\rho_i < L_s$. Between 160 and 520 G, $\rho_i \sim L_s$.

The response of the plasma was studied as the magnitude of the ratio ρ_i/L_s was varied from 0.55 to 3.39 without affecting the plasma conditions. Frequency spectra are obtained from time-resolved Langmuir probe measurements of the floating potential. The dashed vertical lines (red) in Fig. 2 indicate the B_0 for which a transition in the mode frequency occurs. The logarithm of ω/ω_{ci} is plotted as a function of ρ_i/L_s in Fig. 3 to show the three distinct frequency modes observed in the plasma. For reference, under these operating conditions, $f_{ci} = \omega_{ci}/2\pi$ ranges from 3.6 to 22.5 kHz as a function of increasing B_0. When ρ_i/L_s is between 0.55 and 0.62 (corresponding to a high B_0), the mode frequency (~2 kHz) is much smaller than f_{ci}, and the mode frequency (~50 kHz) is much higher than f_{ci} when ρ_i/L_s is between 2.04 and 3.39 (corresponding to a low B_0). If ρ_i/L_s is between 0.64 and 1.85, the mode frequency (~15 kHz) is comparable to f_{ci}.

Figure 4 shows a frequency spectrum and a radial wave power profile for one example from each frequency regime. The ratio of ρ_i/L_s increases going from the top row (a) and (b) to the bottom row (e) and (f). In the radial

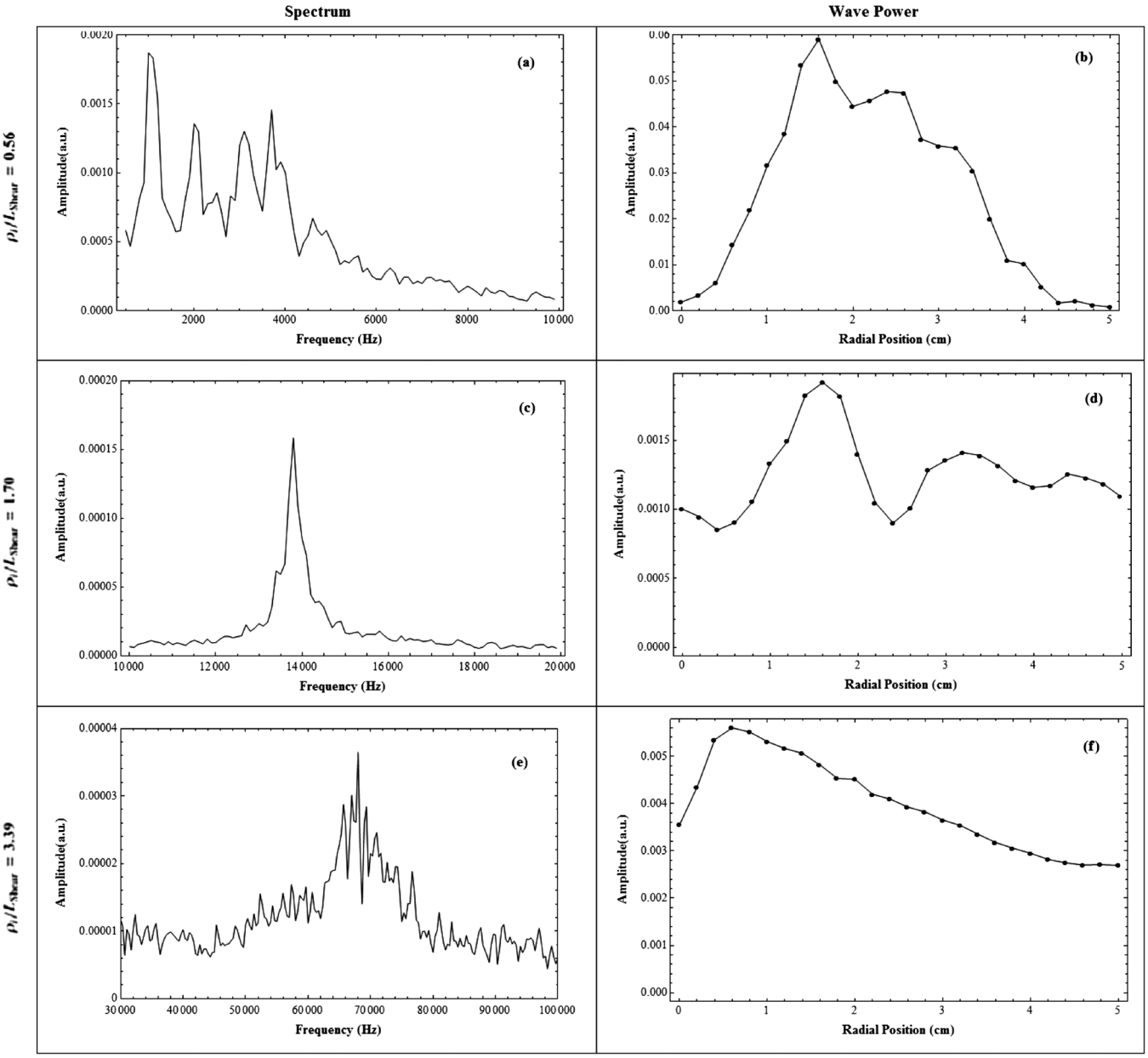

FIG. 4. The FFT spectra and wave power profiles are shown for when (a),(b) $\rho_i < L_s$, (c),(d) $\rho_i \sim L_s$, and (e),(f) $\rho_i > L_s$. The magnetic field strength decreases moving down the columns.

wave power profiles, 0 cm denotes the center of the plasma column and 5 cm corresponds to the edge of the vacuum vessel.

Figures 4(a) and 4(b) show the spectrum and wave power profile for a ρ_i/L_s of 0.56. This spectrum is a very typical case of what is observed when $\rho_i < L_s$. The instability is located at a low frequency so that $\omega/\omega_{ci} = 0.11$. The wave power profile shows that the instability extends over the entire plasma column, peaking at 1.6 cm. There is a radially outward electric field with a peak value of 16 V/cm located at 1.8 cm. The parallel and perpendicular wave number components, k_z and k_y, respectively (relative to the background axial B_0), are measured to be 7.99 and 137.46 m^{-1}, respectively, with a ratio of $k_z/k_y = 0.058$. These signatures are consistent with the Kelvin-Helmholtz mode [39,40].

Figures 4(c) and 4(d) show the spectrum and wave power profile for a measured ρ_i/L_s of 1.70. The spectrum for this case is extremely localized in frequency space and shows that the instability has a much higher frequency ($\omega/\omega_{ci} = 1.9$). The wave power profile shows that the instability is also more localized in space, peaking at 1.6 cm. A radially inward electric field, with a peak strength of 10.5 V/cm is measured in the plasma. The parallel and perpendicular components of the wave number were measured to be 15.55 and 112.76 m^{-1}, respectively, i.e., $k_z/k_y = 0.14$. This is indicative of the IEDDI mechanism [41].

Finally, Figs. 4(e) and 4(f) show the frequency spectrum and wave power profile when $\rho_i/L_s = 3.39$. The instability is localized for $\omega \gg \omega_{ci}$ ($\omega/\omega_{ci} = 14.5$) but close to the lower hybrid frequency ($\omega/\omega_{\mathrm{LH}} = 0.17$). The wave power profile shows that the amplitude peaks near 0.6 cm and is localized near the boundary of the filament and rf plasmas where the velocity shear is localized with a peak electric field of 40 V/cm. The measured perpendicular and parallel wavenumber components are 86.7 and 10.42 m^{-1}, respectively, i.e., $k_z/k_y = 0.12$. This mode has been identified as the EIH mode. Simulations [39] showed that for the EIH mode, $k_z/k_y \sim 0.18$. In a uniform density, the mode frequency is near ω_{LH}. However, theory has shown that the presence of a density gradient can decrease the frequency such that $\omega/\omega_{\mathrm{LH}} < 1$ [14,31]. A mild density gradient (with respect to the electric field gradient), was measured at $r = 0.6$ cm so that the ratio of the diamagnetic drift frequency (ω^*) to the shear frequency is $\omega^*/\omega_s = (k_y V_d)/(V_{E\times B}/L_s) \approx 0.06$ where V_d is the diamagnetic drift velocity and $V_{E\times B}$ is the velocity shear.

In summary, we have reported the first experimental data indicating that a stressed, collisionless plasma can relax through wave emission in a very broad frequency range. Three distinct modes with a spread over 5 orders of magnitude in frequency (normalized by ω_{ci}) arise when ρ_i/L_s is varied by a factor of 7. This is representative of the compression phase of the plasma sheet boundary layer during the onset of disturbed conditions in the magnetosphere. As ρ_i transitions from a value less than L_s to a value comparable to L_s, the mode in the system goes from a frequency less than ω_{ci} to near ω_{ci}. As ρ_i/L_s increases more, the mode frequency rises further into the lower hybrid regime. There may be some mixture of the modes due to overlap of the boundaries of validity. In a small laboratory device like ALEXIS it is difficult to access the ideal regimes for the different modes defined by $1 \ll \rho_i/L_s$, $\rho_i/L_s \sim O(1)$, and $\rho_i/L_s \ll 1$ while keeping other parameters nearly unchanged. But within the practical limitations the transition between the modes is quite clear in our experiment. The results of this work confirm the basic theory that plasma is unstable to localized transverse velocity shear in a very broad frequency range. These results also provide evidence for the theory described by Ganguli *et al.* [3], which proposes that as a compressed boundary layer relaxes in a collisionless plasma it leads to a broadband electrostatic noise signature that satellites have often observed while crossing magnetopsheric boundary layers.

This work is supported by the Defense Threat Reduction Agency (Grant No. HDTRA1-10-1-0019) and the Department of Energy—Office of Fusion Energy Sciences (Grant No. DE-FG02-00ER54476).

[1] G. Ganguli, Y. C. Lee, and P. J. Palmadesso, Phys. Fluids **31**, 823 (1988).
[2] G. Ganguli, Y. C. Lee, and P. J. Palmadesso, Phys. Fluids **31**, 2753 (1988).
[3] G. Ganguli, M. J. Keskinen, H. Romero, R. Heelis, T. Moore, and C. Pollock, J. Geophys. Res. **99**, 8873 (1994).
[4] T. E. Moore, M. O. Chandler, C. J. Pollock, D. L. Reasoner, R. L. Amoldy, and B. Austin, J. Geophys. Res. **101**, 5279 (1996).
[5] D. A. Gurnett, R. R. Anderson, B. T. Tsurutani, E. J. Smith, G. Paschmann, G. Haerendel, S. J. Bame, and C. T. Russell, J. Geophys. Res. **84**, 7043 (1979).
[6] M. Andre, R. Behlke, J. E. Wahlund, A. Vaivads, A. I. Eriksson, A. Tjulin, T. D. Carozzi, C. Cully, G. Gustafsson, and D. Sundkvist, Ann. Geophys. **19**, 1471 (2001).
[7] G. K. Parks, M. McCarthy, R. J. Fitzenreiter, J. Etcheto, K. A. Anderson, R. R. Anterson, T. E. Eastman, L. A. Frank, D. A. Gurnett, C. Huang, R. P. Lin, A. T. Y. Lui, K. W. Ogilvie, A. Pedersen, H. Reme, and D. J. Williams, J. Geophys. Res. **89**, 8885 (1984).
[8] K. Sigsbee, C. A. Cattell, F. S. Mozer, K. Tsuruda, and S. Kokubun, J. Geophys. Res. **106**, 435 (2001).
[9] T. Streed, C. Cattell, F. Mozer, S. Kokubun, and K. Tsuruda, J. Geophys. Res. **106**, 6275 (2001).
[10] W. A. Scales, P. A. Bernhardt, and G. Ganguli, J. Geophys. Res. **100**, 269 (1995).
[11] G. Ganguli, P. A. Bernhardt, W. A. Scales, P. Rodriguez, C. L. Siefring, and H. Romero, *Physics of Space Plasmas,*

SPI Conf. Proc. and Reprint Series (Scientific Publishers Inc., Cambridge, MA, 1992), p. 161.
[12] P. A. Bernhardt, P. Rodriguez, C. L. Siefring, and C. S. Lin, J. Geophys. Res. **96**, 13 887 (1991).
[13] H. Romero, G. Ganguli, P. J. Palmadesso, and P. B. Dusenbery, Geophys. Res. Lett. **17**, 2313 (1990).
[14] H. Romero, G. Ganguli, Y. C. Lee, and P. J. Palmadesso, Phys. Fluids B **4**, 1708 (1992).
[15] P. M. Kintner, J. Bonnell, R. Arnoldy, K. Lynch, M. Hall, C. Pollock, T. Moore, J. Holtet, C. Deehr, H. Stenbaek-nielsen, R. Smith, and J. Olson, Geophys. Res. Lett. **23**, 1865 (1996).
[16] C. S. Lakhina, J. Geophys. Res. **92**, 12 161 (1987).
[17] H. Romero and G. Ganguli, Geophys. Res. Lett. **21**, 645 (1994).
[18] H. Romero, G. Ganguli, and Y. C. Lee, Phys. Rev. Lett. **69**, 3503 (1992).
[19] W. E. Amatucci, J. Geophys. Res. **104**, 14 481 (1999).
[20] G. I. Kent, N. C. Jen, and F. F. Chen, Phys. Fluids **12**, 2140 (1969).
[21] D. L. Jassby, Phys. Rev. Lett. **25**, 1567 (1970).
[22] D. L. Jassby, Phys. Fluids **15**, 1590 (1972).
[23] M. Cianciosa, Ph.D. Dissertation, Auburn University, 2012.
[24] M. E. Koepke, W. E. Amatucci, J. J. Carroll, and T. E. Sheridan, Phys. Rev. Lett. **72**, 3355 (1994).
[25] M. E. Koepke, J. J. Carroll, and M. W. Zintl, Phys. Plasmas **5**, 1671 (1998).
[26] W. E. Amatucci, M. E. Koepke, J. J. Carroll, and T. E. Sheridan, Geophys. Res. Lett. **21**, 1595 (1994).
[27] W. E. Amatucci, D. N. Walker, G. Ganguli, J. A. Antoniades, D. Duncan, J. H. Bowles, V. Gavrishchaka, and M. E. Koepke, Phys. Rev. Lett. **77**, 1978 (1996).
[28] W. E. Amatucci, D. N. Walker, G. Ganguli, D. Duncan, J. A. Antoniades, J. H. Bowles, V. Gavrishchaka, and M. E. Koepke, J. Geophys. Res. **103**, 11 711 (1998).
[29] E. Thomas, J. D. Jackson, E. A. Wallace, and G. Ganguli, Phys. Plasmas **10**, 1191 (2003).
[30] A. C. Eadon, Ph.D. Dissertation, Auburn University, 2011.
[31] W. E. Amatucci, G. Ganguli, D. N. Walker, G. Gatling, M. M. Balkey, and T. McCulloch, Phys. Plasmas **10**, 1963 (2003).
[32] A. Matsubara and T. Tanikawa, Jpn. J. Appl. Phys. **39**, 4920 (2000).
[33] T. A. Santhosh Kumar, S. K. Mattoo, and R. Jha, Phys. Plasmas **9**, 2946 (2002).
[34] G. Ganguli, Phys. Plasmas **4**, 1544 (1997).
[35] E. A. Wallace, E. Thomas, A. C. Eadon, and J. D. Jackson, Rev. Sci. Instrum. **75**, 5160 (2004).
[36] A. C. Eadon, E. M. Tejero, A. M. DuBois, and E. Thomas, Rev. Sci. Instrum. **82**, 063511 (2011).
[37] A. M. DuBois, I. Arnold, E. Thomas, E. M. Tejero, and W. E. Amatucci, Rev. Sci. Instrum. **84**, 043503 (2013).
[38] W. B. Nottingham, Phys. Rev. Lett. **49**, 78 (1936).
[39] H. Romero and G. Ganguli, Phys. Fluids B **5**, 3163 (1993).
[40] H. Hojo, Y. Kishimoto, and J. W. Van Dam, J. Phys. Soc. Jpn. **64**, 4073 (1995).
[41] J. R. Peñano, G. Ganguli, W. E. Amatucci, D. N. Walker, V. Gavrishchaka, and J. R. Peñano, Phys. Plasmas **5**, 4377 (1998).